



Comparison of the reproducibility of 2D and 3D amide proton transfer weighted imaging in intracranial rat gliomas at 3 T

Xin Chen¹ · Xinhua Wei¹ · Lingling Liu¹ · Xu Yan² · Xiaolei Zhu³ · Xiangdong Xu¹ · Xinqing Jiang¹ · Zaiyi Liu⁴

Received: 24 September 2019 / Revised: 29 January 2020 / Accepted: 17 February 2020 / Published online: 10 March 2020
© Springer Nature Singapore Pte Ltd. 2020

Abstract

Magnetic resonance-based amide proton transfer weighted (APT_w) imaging is one subset of the chemical exchange saturation transfer (CEST) imaging techniques and could provide a potential novel tool of tumor detection and characterization. The purpose of this study was to compare the reproducibility of APT_w imaging with two-dimensional (2D) and three-dimensional (3D) techniques in rat intracranial gliomas. Thirty-two Sprague–Dawley (SD) male rats bearing intracranial C6 glioma underwent 2D and 3D APT_w imaging twice with a 3 T scanner, respectively. Paired *t* test was used to compare the difference of magnetization transfer ratio asymmetry (MTR_{asym}) values obtained from 2D and 3D APT_w images with respect to tumor and the contralateral normal-appearing brain tissue. The reproducibility of MTR_{asym} measurement values was evaluated using Bland–Altman plot. Our results showed that the reproducibility of MTR_{asym} measurement values from 3D APT_w imaging is superior to 2D APT_w technique. Therefore, 3D APT_w imaging for the brain tumor would be recommended to use in clinical practice with a clinically relevant time frame and research works considering the good reproducibility compared to 2D APT_w imaging.

Keywords Glioma · Magnetic resonance imaging · Amide proton transfer weighted imaging · Reproducibility

Introduction

Magnetic resonance-based amide proton transfer weighted (APT_w) imaging is one subset of the chemical exchange saturation transfer (CEST) imaging techniques initially introduced by Zhou and van Zijl et al. [1, 2]. APT can detect the saturation transfer efficiency owing to chemical exchange

between bulk-water protons and endogenous mobile proteins. Thus, it is sensitive to the concentration of amide protons associated with the containing protein/peptide and could provide a potential novel tool for tumor detection and characterization [1, 3]. Recently, APT_w imaging has been demonstrated to provide valuable information for brain tumors at 3 T [4]. Previous studies showed that APT_w imaging was able to grade brain tumors [5, 6], distinguish glioma recurrence from radiation necrosis [7], and also predict the clinical outcome of brain diseases [8, 9].

Although previous works have demonstrated the substantial impact of APT_w imaging on patient management [5], its reproducibility is extremely important for reliable quantification in the clinical scenario. In terms of APT_w acquisition techniques, both two-dimensional (2D) and three-dimensional (3D) gradient-echo readouts are available CEST sequences [10–13]. While owing to the feature of CEST imaging acquisition, both techniques have their own advantages. With 2D readout, the shorter acquisition time is preferred in clinical settings, while it suffers the drawbacks of less volume coverage with only one single-slice acquisition [14]. With 3D readout, it could cover the whole brain with multi-slice imaging and minimize relaxation loss

Xin Chen and Xinhua Wei contributed equally.

✉ Xinqing Jiang
jiangxqw@163.com

✉ Zaiyi Liu
zylu@163.com

¹ Department of Radiology, Guangzhou First People's Hospital, School of Medicine, South China University of Technology, Guangzhou 510180, China

² MR Collaboration NE Asia, Siemens Healthcare, Shanghai, China

³ Radiology, Bayer Healthcare, Guangzhou, China

⁴ Department of Radiology, Guangdong Provincial People's Hospital, Guangdong Academy of Medical Sciences, 106 Zhongshan Er Road, Guangzhou 510080, China

between slices [15], while longer acquisition time is needed. Recently, a 3D gradient and spin-echo (GRASE)-based sequence was proposed to improve the contrast-to-noise ratio with shorter acquisition time [16], which makes it possible for 3D APTw imaging to perform in clinical practice.

Although 2D and 3D APTw acquisitions have their own advantages, the reproducibility of the quantitative parameter calculated from APTw imaging is extremely important for clinical application. Therefore, the purpose of this study was to compare the reproducibility of magnetization transfer ratio asymmetry (MTR_{asym}) calculated from APTw imaging of intracranial rat gliomas with 2D and 3D sequences at 3T.

Materials and methods

Animal preparation

The animal experiment was approved by our hospital's Institutional Animal Care and Use Committee. Thirty-four Sprague–Dawley (SD) male rats weighing 200–250 g were obtained from the Guangdong Medical Laboratory Animal Center. The rat C6 glioma cells were harvested by trypsinization, washed once with Hanks' balanced salt solution (HBSS), and a cell suspension containing 5×10^5 cells in a volume of 10 μl of HBSS over 10 min was used for implantation into the striatum of rat brains. The SD male rats were cared for throughout the experimental procedures following the institutional guidelines. The rats were anesthetized by intraperitoneal injection of 0.3 ml/kg body weight of 10% chloral hydrate. Rats under anesthesia were placed in a small animal stereotactic frame (David Kopf Instruments, Tujunga, CA). A sagittal incision was made through the skin to expose the cranium, and a burr hole was made in the skull at 0.5 mm anterior and 3 mm lateral from bregma using a small dental drill. The needle was initially advanced to a depth of 6 mm and then withdrawn to a depth of 5 mm to limit reflux up the needle track. Ten microliters of C6 glioma cell suspension were injected at a rate of 1 $\mu\text{l}/\text{min}$. After inoculation and a wait of 5 min, the needle was removed, and the wound was closed with sutures.

MRI experiments

All rats with 1 week later post-implantation of C6 glioma cells underwent MR imaging at a 3.0 T scanner (MAGNETOM Verio Siemens Healthcare, Erlangen, Germany) using a four-channel phased-array animal coil (inner diameter = 5 cm). The MR scan consisted of T_2 -weighted sequences in sagittal and coronal orientation (repetition time = 3500 ms; echo time = 88 ms; slices = 20 for coronal scan and 15 for sagittal scan; FOV = 64 mm \times 64 mm; slice thickness = 0.9 mm), a prototype sequence for 2D APTw

imaging in coronal orientation was performed on a single slice with a maximum cross-sectional area of the tumor (TR = 1180 ms; TE = 3.14 ms; FOV = 71 mm \times 95 mm; in-plane resolution = 0.5 mm \times 0.5 mm; slice thickness = 3 mm), and 3D APTw Imaging were also executed with the entire brain (TR = 16 ms; TE = 4.05 ms; FOV = 49 mm \times 60 mm \times 32 mm; resolution = 0.5 mm \times 0.5 mm \times 2 mm). After the first scan, each rat bearing tumor was removed from the imager and then relocated for a second scan including both 2D and 3D APTw images acquisition. The same parameters were used for repeated APTw imaging.

In this study, 2D APTw imaging was performed with gradient echo sequence, nineteen-offset APT data (± 4.2 , ± 3.7 , ± 3.3 , ± 2.8 , ± 2.3 , ± 1.9 , ± 1.4 , ± 0.9 , ± 0.5 , 0 ppm, applied saturation power 1.5 μT) with a reference without pre-saturation were acquired. The 2D APTw MRI lasted for about 3 min. The 3D APTw imaging was performed with 3D radiofrequency (RF)-spoiled gradient-echo sequence with a pre-saturation module for selective saturation of resonance signals and GRAPPA acceleration by a factor of 2. Seventeen datasets with presaturation at different offset frequencies ($\Delta\omega$ (± 5.0 , ± 4.4 , ± 3.8 , ± 3.1 , ± 2.5 , ± 1.9 , ± 1.3 , ± 0.6 , 0 ppm, applied saturation power 1.5 μT) from the bulk water resonance (M_{sat}) and one reference without pre-saturation were acquired during one experiment. The total scan time of 3D APTw imaging was about 11 min.

Imaging analysis

The datasets were processed on Siemens Workstation, with similar procedures described in previous work [17]. First, the standard z -spectra (residual magnetization after selective pre-saturation) was normalized by the signal of the reference image (M_0) and plotted against the saturation offset frequency ($\Delta\omega$). Then a voxel-by-voxel correction of B_0 heterogeneities was applied and the minimum of z -spectra was determined and shifted to $\Delta\omega = 0$, which was assumed to be the corresponding resonance frequency of bulk water protons. Second, APT effects were calculated from the z -spectra by referencing the saturated magnetization at the amide proton frequency ($\Delta\omega = 3.5$ ppm) in comparison to its saturated magnetization at $\Delta\omega = -3.5$ ppm. The values of magnetization transfer ratio asymmetry ($MTR_{\text{asym}}(\Delta\omega) = M_{\text{sat}}(-\Delta\omega) - M_{\text{sat}}(\Delta\omega)/M_0$) at the offset of the amide proton frequency could reflect the pixel intensities of APTw images.

The images independently were reviewed by two radiologists (X.C. and X.W.) with, respectively, 7 years and 15 years neuro-experience, respectively. APTw imaging features were evaluated within regions of abnormality shown on conventional MRI sequences. For 3D images, a single slice corresponding to the 2D APTw images was chosen for quantitative measurement. Two regions of interest (ROIs)

for tumor (Fig. 1) and contralateral normal-appearing brain tissue were drawn manually on the APTw images according to the T₂-weighted imaging.

Statistical analysis

MTR_{asym} values were expressed as mean ± standard deviation (SD). The Kolmogorov–Smirnov test was used for normality and the Levene test for homogeneity of variances. Intra- and inter-observer agreement of MTR_{asym} measurement was evaluated using the intraclass correlation coefficients (ICCs). Intra-observer agreement was evaluated using reader 1’s two measurements, and the data for the inter-observer ICC calculation was from reader 1’s first measurements and reader 2’s measurements. An ICC greater than 0.75 was considered to be good agreement [18].

To evaluate the systematic bias of repeated MTR_{asym} values, the values of MTR_{asym} were compared between the two-repeated series using a paired-sample *t* test for 2D and 3D APTw images, respectively. A paired-sample *t* test was used to evaluate the differences of MTR_{asym} between tumor and contralateral normal-appearing brain tissue and the differences between 2D and 3D APTw images for tumor and contralateral normal-appearing brain tissue, respectively.

The reproducibility of MTR_{asym} values from 2D to 3D APTw imaging was evaluated by the Bland–Altman method. The mean absolute difference (bias) and 95% confidence interval of the mean difference (limits of agreement [LOAs]) between the first and second APTw imaging series were compared.

Statistical analyses were performed using MedCalc (MedCalc, Mariakerke, Belgium) software for Windows. *P* < 0.05 was considered significantly statistical difference.

Results

Intra- and inter-observer agreement of MTR_{asym} measurement

Two rats failed to develop a tumor based on the MR images. Thus, data from 32 rats with glioma were evaluated in our study. The intra-observer ICC calculated based on reader 1’s two measurements ranged from 0.871 to 0.920 (Table 1). Inter-observer agreement between reader 1’s first measurements and reader 2’s measurements was good with ICCs ranging from 0.771 to 0.852 (Table 1). The intra- and inter-observer reproducibility of the MTR_{asym} measurement

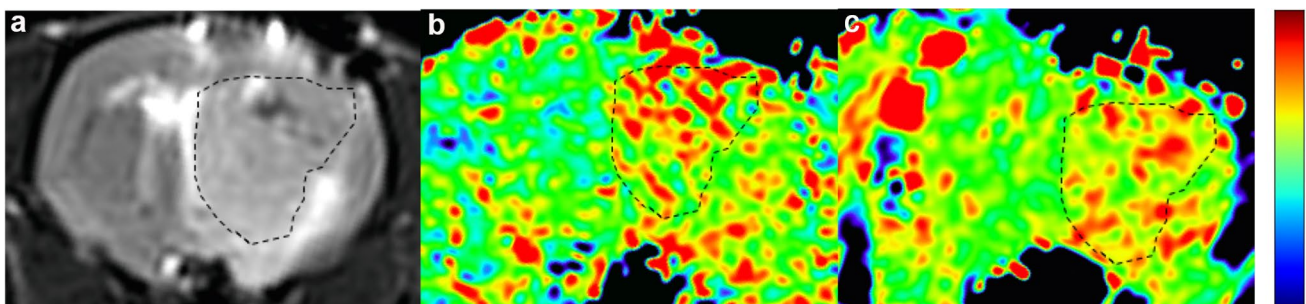


Fig. 1 In-vivo APT weighted imaging of C6 glioma in the orthotopic mouse model. Representative T2-weighted images (a) and APT weighted images with 2D (b) and 3D scans (c) (MTR_{asym} map

at 3.5 ppm) where the tumors were delineated brighter than the contralateral normal-appearing brain tissue

Table 1 Inter- and intra-observer agreements for values of all MTR_{asym}

Series	2D		3D	
	Glioma	Normal	Glioma	Normal
First				
Intra-	0.911 (0.817, 0.956)	0.871 (0.735, 0.937)	0.918 (0.832, 0.960)	0.888 (0.771, 0.945)
Inter-	0.836 (0.670, 0.916)	0.771 (0.581, 0.881)	0.848 (0.712, 0.923)	0.799 (0.627, 0.896)
Second				
Intra-	0.893 (0.780, 0.948)	0.902 (0.799, 0.952)	0.920 (0.836, 0.961)	0.895 (0.786, 0.949)
Inter-	0.806 (0.640, 0.900)	0.821 (0.665, 0.906)	0.852 (0.718, 0.925)	0.811 (0.647, 0.903)

Data in parentheses are 95% confidence intervals

Inter- inter-observer agreements, *intra-* intra-observer agreements, *2D* two-dimensional APT weighted technique, *3D* three-dimensional APT weighted technique

values was good. Therefore, further analysis was based on the data from read 1' first measurement.

MTR_{asym} value of tumor and contralateral normal-appearing brain tissue with 2D and 3D APTw images

Table 2 shows the comparison of MTR_{asym} values of tumor and contralateral normal-appearing brain tissue. The means MTR_{asym} values of tumor (2D 1.721–1.739%; 3D 0.777–0.909%) were significantly higher than those of contralateral normal-appearing brain tissue (2D 0.358–0.476%; 3D 0.050 to –0.005%) with either 2D or 3D APTw imaging ($P < 0.001$).

MTR_{asym} of tumor and contralateral normal-appearing brain tissue from 2D APTw images were significantly larger than those with 3D APTw images on both tumor and contralateral brain tissue ($P < 0.001$).

Reproducibility of MTR_{asym} measurement in tumor and contralateral normal-appearing brain tissue with 2D and 3D APTw sequences

The reproducibility of MTR_{asym} measurement of both tumor and contralateral normal-appearing brain tissue with 3D APTw imaging were better than those with 2D APTw technique (Fig. 2). For example, the LOA between the two repeated APTw imaging in tumor with 2D scan was -0.020 ± 0.870 , while the LOA was 0.130 ± 0.470 for 3D scan.

For both 2D and 3D APTw imaging, the reproducibility of MTR_{asym} measurement in tumor was inferior to that in contralateral normal-appearing brain tissue. For example, the LOA between the two repeated APTw imaging in tumor with 3D scan was 0.130 ± 0.470 , while the LOA in contralateral normal-appearing brain tissue with 3D scan was 0.030 ± 0.315 .

Discussion

Our results showed that the reproducibility of MTR_{asym} measurement with 3D APTw imaging was superior to 2D sequence, while the MTR_{asym} values obtained with 2D APTw imaging were higher than those with 3D scan for both tumor and contralateral normal-appearing brain tissue. Meanwhile, the MTR_{asym} measurement of tumor showed significantly higher values and poorer reproducibility than that of the contralateral normal-appearing brain tissue for both 2D and 3D APTw imaging.

Signal-to-noise ratio (SNR) is a vital factor in consistent APTw imaging [19]. Improvement in quantifying the APT effect is expected with an increased SNR. A precious study comparing APT measurements at 7 T with those at 3 T showed that these measurements at 3 T were more variable partly because of the high SNR at 7 T [20]. In our study, we compared the reproducibility of MTR_{asym} measurement for 3D APTw imaging with that for 2D APTw sequence and found that the MTR_{asym} with 3D APTw imaging had a better reproducibility than that with 2D technique in both tumor and contralateral normal-appearing brain tissue. This may be due to higher SNR of 3D APTw imaging with volume excitation and better excitation homogeneity [15, 21]. In addition, APTw quantification and image appearance could be affected by competing saturation phenomena such as direct water saturation and the images near the ventricle. And 2D APTw imaging is more likely influenced by direct water saturation than 3D APTw imaging [12]. These may account for the poorer reproducibility of MTR_{asym} using 2D APTw imaging.

In addition, we found that MTR_{asym} was higher in 2D APTw imaging compared to 3D scan. It is not expected that the concentration or exchange rate differs as the function of 2D or 3D readout; therefore, these phenomena may be related to a sensitivity difference, the sequence parameters or a relatively reduced inclusion of magnetization transfer (MT) effect. Meanwhile, we also speculated that this elevation in 2D APTw imaging might result from the direct water

Table 2 The comparison of values of all MTR_{asym}

	First			Second		
	2D	3D	P*	3D	2D	P*
Glioma	1.739 ± 0.516	0.909 ± 0.374	< 0.001	0.777 ± 0.434	1.721 ± 0.487	< 0.001
Normal	0.358 ± 0.242	-0.005 ± 0.235	< 0.001	-0.050 ± 0.244	0.476 ± 0.354	< 0.001
P#	< 0.001	< 0.001		< 0.001	< 0.001	

Data are mean ± standard deviation

First the first series of APT weighted images acquisition, Second the second series of APT weighted images acquisition, 2D two-dimensional APT weighted techniques, 3D three-dimensional APT weighted techniques

*Paired *t* test revealed significant differences in MTR_{asym} between 2D and 3D APT weighted techniques

#Paired *t* test revealed significant differences in MTR_{asym} of tumor and the normal-appearing brain tissues

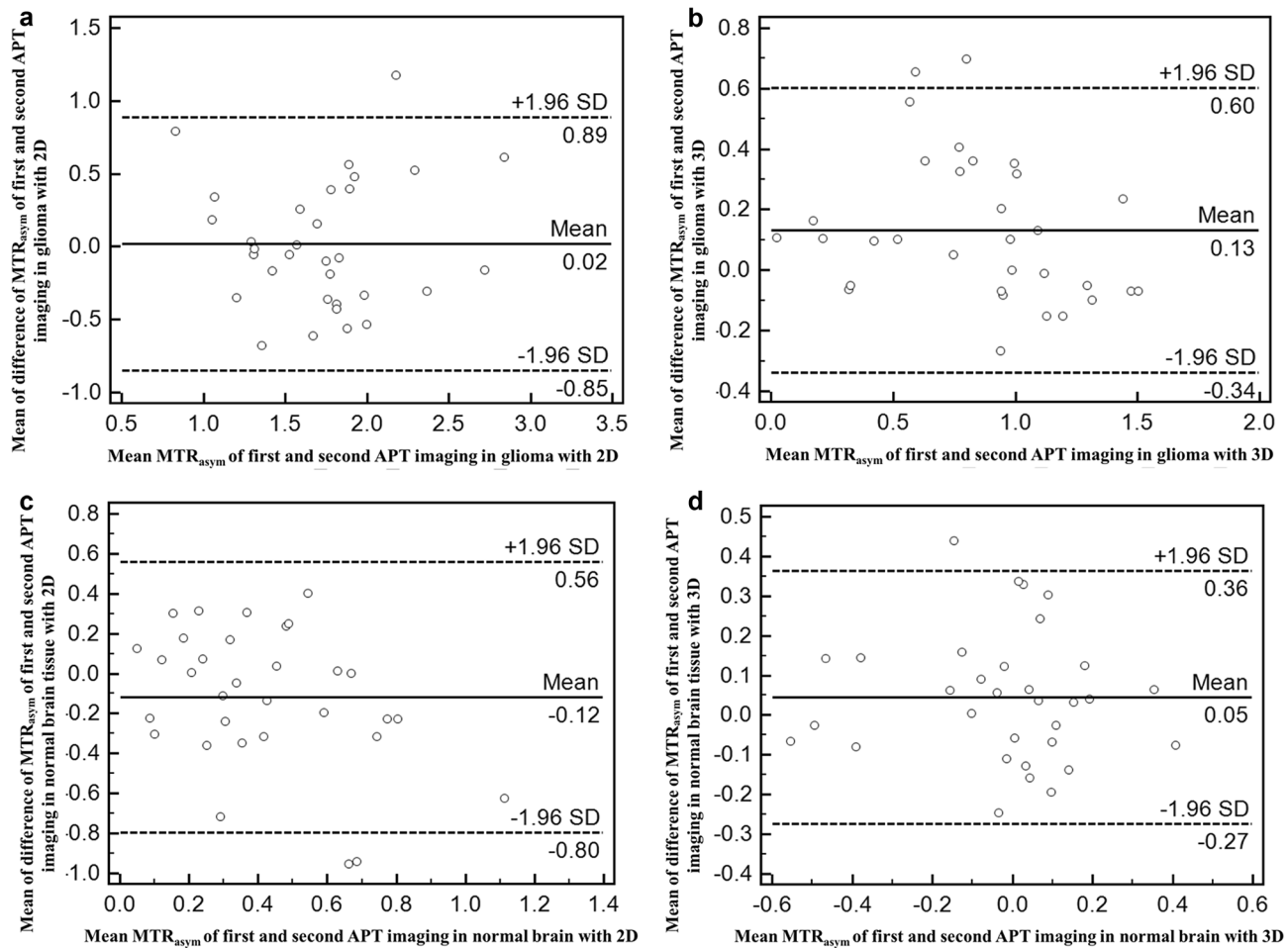


Fig. 2 Bland-Altman plots show reproducibility of MTR_{asym} (%) in glioma and the contralateral normal-appearing brain tissue with 2D and 3D scans: **a** glioma with 2D and 3D (**b**), **c** the contralateral

normal-appearing brain tissue with 2D and 3D (**d**). Blue line = mean absolute difference, red lines = 95% confidence interval of the mean difference (LOA)

saturation which may result in more significant overlap of resonances that could artificially inflate the observed APT effect [20].

The APT signal is measured through the MTR_{asym} at ± 3.5 ppm, so the APTw imaging signal in tissue is mainly related to the increased mobile amide proton content and increased intracellular pH in the tumor [22–24]. Because only a small pH increase of intracellular (around 0.1 pH unit) is detected in brain tumor and the normal-appearing brain tissue [5, 25], the increased APT effect in brain tumor may be attributed to the increased amide proton concentration [26]. Meanwhile, Yan et al. [27] investigated the biochemical origin of the APT weighted hyper-intensity in brain tumors and confirmed an increase in the cytosolic protein concentration in tumors, furthermore, identified several key proteins that may cause APT weighted hyper-intensity compared to normal brain regions. Heo et al. [28] also found that the MTR_{asym} signal of glioma was significantly higher than those of normal brain regions. Similar to these findings, our

results also showed that the tumor had significantly higher MTR_{asym} than those in the contralateral normal-appearing brain tissue.

To our knowledge, there is no data available regarding the reproducibility of MTR_{asym} measurements in brain tumor and contralateral normal-appearing brain tissue. While we found that the reproducibility of MTR_{asym} measurements in brain tumor was poorer than that in contralateral normal-appearing brain tissue, which might be explained by the higher heterogeneity in brain tumor compared to normal-appearing brain tissue [29].

There are several limitations in our study. First, there is no real reference standard for APTw signal, while the reproducibility of a newly developed quantitative parameter MTR_{asym} is vital compared to the true values for clinical applications. Second, the number of rats in this study are small. Thirdly, we only compared and evaluated the reproducibility of MTR_{asym} values from intracranial rat glioma without therapy. It should be noticed that the results in glioma between

with and without therapy may differ, because the glioma after therapy may have a more heterogeneous tumor micro-environment. Finally, the imaging parameters of 2D and 3D CEST sequences are slightly different, such as saturation frequencies.

In conclusion, we demonstrated a good reproducibility of 3D APTw imaging of brain tumors. We recommend that MTR_{asym} measurement of the brain tumor can be performed with 3D APTw imaging in clinical practice with a clinically relevant time frame and research works considering the good reproducibility and multi-slice acquisition compared to 2D APTw imaging.

Acknowledgements This work was partly supported by the National Key Research and Development Program of China (Grant no 2017YFC130910002), the National Science Foundation of China (Grant no. 81601469, 81771912 and 81871846) and Guangzhou Science and Technology Project of Health (no. 20191A011002).

References

- Zhou J, Payen JF, Wilson DA, et al. Using the amide proton signals of intracellular proteins and peptides to detect pH effects in MRI. *Nat Med*. 2003;9:1085–90.
- Zhou J, Lal B, Wilson DA, et al. Amide proton transfer (apt) contrast for imaging of brain tumors. *Magn Reson Med*. 2003;50:1120–6.
- Zaiss M, Bachert P. Chemical exchange saturation transfer (CEST) and MR Z-spectroscopy in vivo: a review of theoretical approaches and methods. *Phys Med Biol*. 2013;58:R221–69.
- Zhou J, Heo HY, Knutsson L, et al. APT-weighted MRI: techniques, current neuro applications, and challenging issues. *J Magn Reson Imaging*. 2019;50:347–64.
- Park JE, Kim HS, Park KJ, et al. Histogram analysis of amide proton transfer imaging to identify contrast-enhancing low-grade brain tumor that mimics high-grade tumor: increased accuracy of MR perfusion. *Radiology*. 2015;277:151–61.
- Zhang J, Zhu W, Tain R, et al. Improved differentiation of low-grade and high-grade gliomas and detection of tumor proliferation using APT contrast fitted from Z-spectrum. *Mol Imaging Biol*. 2018;20:623–31.
- Zhou J, Tryggstad E, Wen Z, et al. differentiation between glioma and radiation necrosis using molecular magnetic resonance imaging of endogenous proteins and peptides. *Nat Med*. 2011;17:130–4.
- Lin G, Zhuang C, Shen Z, et al. APT weighted MRI as an effective imaging protocol to predict clinical outcome after acute Ischemic stroke. *Front Neurol*. 2018;9:901.
- Paech D, Dreher C, Regnery S, et al. Relaxation-compensated amide proton transfer (APT) MRI signal intensity is associated with survival and progression in high-grade glioma patients. *Eur Radiol*. 2019;29:4957–67.
- Sun PZ, Murata Y, Lu J, et al. relaxation-compensated fast multi-slice amide proton transfer (apt) imaging of acute ischemic stroke. *Magn Reson Med*. 2008;59:1175–82.
- Sun PZ, Cheung JS, Wang E, et al. Fast multislice pH-weighted chemical exchange saturation transfer (cest) mri with unevenly segmented rf irradiation. *Magn Reson Med*. 2011;65:588–94.
- Jones CK, Polders D, Hua J, et al. In vivo three-dimensional whole-brain pulsed steady-state chemical exchange saturation transfer at 7 T. *Magn Reson Med*. 2012;67:1579–89.
- Khlebnikov V, Siero JCW, Bhogal AA, et al. Establishing upper limits on neuronal activity-evoked pH changes with APT-CEST MRI at 7 T. *Magn Reson Med*. 2018;80:126–36.
- Togao O, Hiwatashi A, Keupp J, et al. Scan-rescan reproducibility of parallel transmission based amide proton transfer imaging of brain tumors. *J Magn Reson Imaging*. 2015;42:1346–53.
- Zhu H, Jones CK, van Zijl PC, et al. Fast 3d chemical exchange saturation transfer (cest) imaging of the human brain. *Magn Reson Med*. 2010;64:638–44.
- Yoshida M, Nakaura T, Inoue T, et al. Magnetic resonance cholangiopancreatography with GRASE sequence at 3.0 T: does it improve image quality and acquisition time as compared with 3D TSE? *Eur Radiol*. 2018;28:2436–43.
- Haneder S, Apprich SR, Schmitt B, et al. Assessment of glycosaminoglycan content in intervertebral discs using chemical exchange saturation transfer at 3.0 Tesla: preliminary results in patients with low-back pain. *Eur Radiol*. 2013;23:861–8.
- Shrout PE, Fleiss JL. Intraclass correlations: uses in assessing rater reliability. *Psychol Bull*. 1979;86:420–8.
- Zhou J, Blakeley JO, Hua J, et al. Practical data acquisition method for human brain tumor amide proton transfer (APT) imaging. *Magn Reson Med*. 2008;60:842–9.
- Klomp DW, Dula AN, Arlinghaus LR, et al. amide proton transfer imaging of the human breast at 7 t: development and reproducibility. *NMR Biomed*. 2013;26:1271–7.
- Khlebnikov V, Polders D, Hendrikse J, et al. Amide proton transfer (APT) imaging of brain tumors at 7 T: the role of tissue water T(1)—relaxation properties. *Magn Reson Med*. 2017;77:1525–32.
- Togao O, Yoshiura T, Keupp J, et al. Amide proton transfer imaging of adult diffuse gliomas: correlation with histopathological grades. *Neuro Oncol*. 2014;16:441–8.
- Tee YK, Harston GW, Blockley N, et al. Comparing different analysis methods for quantifying the MRI amide proton transfer (APT) effect in hyperacute stroke patients. *NMR Biomed*. 2014;27:1019–29.
- Song G, Li C, Luo X, et al. Evolution of cerebral ischemia assessed by amide proton transfer-weighted MRI. *Front Neurol*. 2017;8:67.
- Sakata A, Okada T, Yamamoto A, et al. Grading glial tumors with amide proton transfer MR imaging: different analytical approaches. *J Neurooncol*. 2015;122:339–48.
- Lee D-H, Heo H-Y, Zhang K, et al. Quantitative assessment of the effects of water proton concentration and water T(1) changes on amide proton transfer (APT) and nuclear overhauser enhancement (NOE) MRI: the origin of the APT imaging signal in brain tumor. *Magn Reson Med*. 2017;77:855–63.
- Yan K, Fu Z, Yang C, et al. Assessing amide proton transfer (APT) MRI contrast origins in 9 L gliosarcoma in the rat brain using proteomic analysis. *Mol Imaging Biol*. 2015;17:479–87.
- Heo H-Y, Jones CK, Hua J, et al. Whole-brain amide proton transfer (APT) and nuclear overhauser enhancement (NOE) imaging in glioma patients using low-power steady-state pulsed chemical exchange saturation transfer (CEST) imaging at 7 T. *J Magn Reson Imaging*. 2016;44:41–50.
- Akgul S, Patch AM, D'Souza RCJ, et al. Intratumoural heterogeneity underlies distinct therapy responses and treatment resistance in glioblastoma. *Cancers*. 2019;11:E190.

Publisher's Note Springer Nature remains neutral with regard to jurisdictional claims in published maps and institutional affiliations.